rac-[Methylene(3-*tert*-butyl-1-indenyl)$_2$]ZrCl$_2$: A Simple, High-Performance Zirconocene Catalyst for Isotactic Polypropene

Luigi Resconi,* Davide Balboni, Giovanni Baruzzi, Cristina Fiori, and Simona Guidotti

Montell Polyolefins, Centro Ricerche G. Natta, 44100 Ferrara, Italy

Pierluigi Mercandelli and Angelo Sironi

Dipartimento di Chimica Strutturale e Stereochimica Inorganica, Università di Milano, Via Venezian 21, 20133 Milano, Italy

Received June 25, 1999

The synthesis and propene polymerization performance of the novel *rac*-[CH$_2$(3-*tert*-butyl-1-indenyl)$_2$]ZrCl$_2$ (**2**) and *rac*-[CH$_2$(3-*tert*-butyl-1-indenyl)$_2$]ZrMe$_2$ (**2-Me$_2$**) are described. The ligand precursor, bis(1-*tert*-butyl-3-indenyl)methane (**L2**), is obtained in ca. 80% conversion from the condensation of 3-*tert*-butylindene and formaldehyde in DMF at room temperature and is isolated as a yellow powder by washing with pentane. Red **2** is obtained in 50−60% yield and free from its *meso* stereoisomer by reacting an Et$_2$O solution of the ligand dianion, (**L2**)Li$_2$(Et$_2$O)$_x$, with a slurry of ZrCl$_4$ in either pentane or toluene. Yellow **2-Me$_2$** is prepared in 90% yield by reaction of **2** with excess MeMgCl in toluene. Alternatively, **2-Me$_2$** (contaminated with about 5% of its *meso* isomer) can be obtained directly from the ligand **L2**, by reacting **L2** in Et$_2$O with 4 equiv of MeLi and then 1 equiv of ZrCl$_4$ in toluene. Both **2** and **2-Me$_2$** are remarkably soluble in pentane (**2**, ca. 1.7 g/L; **2-Me$_2$**, ca. 13 g/L) and toluene (**2**, ca. 50 g/L). **2**/MAO and **2-Me$_2$**/MAO polymerize liquid propene with good activities to highly isotactic (*mmmm* = 95−98%), fully regioregular polypropene with medium-high molecular weights ($\bar{M}_w$ = 70 000−780 000) and high melting points (T_m = 154−163 °C) in the T_p range 30−70 °C. The behavior of **2** is compared to that of the prototypical Montell zirconocene *rac*-[Me$_2$C(3-*t*-Bu-Ind)$_2$]ZrCl$_2$ (**1**). **2** is the first example of a highly efficient and at the same time simple and inexpensive zirconocene catalyst for isotactic polypropene. The molecular structures of **2** and its Hf analogue (**Hf-2)** have been determined and compared to that of **1**.

Introduction

The evolution of zirconocene catalysts for the isospecific polymerization of propene[1] has been marked by the increase in performance coupled with increase in synthetic difficulty. So far, to enable better control over stereochemistry, regiochemistry, and chain transfer reactions, indenes would have to be substituted on the least "natural" position, that is the 2- and 4-carbons, a strategy requiring the multistep building of the C-5 ring of the final indene onto the properly substituted benzene.[2]

Recently, we described a new class of C_2-symmetric zirconocenes, of general formula *rac*-R$_2$C(3-R′-Ind)$_2$-ZrCl$_2$, whose performance in propene polymerization strongly depends on the size of the substituent in C(3).[3] The main advantages of these complexes reside on the simple synthesis of single carbon bridged bisindenyl ligands, initially developed by Nifant'ev and co-workers (Scheme 1),[4] and the inactivity of their *meso* isomers in propene polymerization.

Scheme 1

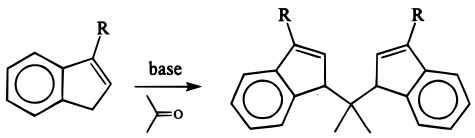

The racemic zirconocenes are fully regiospecific, with isospecificity increasing with the bulkiness of the substituent on C(3): CH$_3$ < Me$_3$Si < *t*-Bu. Indeed the *rac*-[Me$_2$C(3-*tert*-butyl-1-indenyl)$_2$]ZrCl$_2$/MAO catalyst

(1) Brintzinger, H. H.; Fischer, D.; Mülhaupt, R.; Rieger, B.; Waymouth, R. M. *Angew. Chem., Int. Ed. Engl.* **1995**, *34*, 1143−1170.

(2) (a) Mise, T.; Miya, S.; Yamazaki, H. *Chem. Lett.* **1989**, 1853. (b) Roll, W.; Brintzinger, H. H.; Rieger, B.; Zolk, R. *Angew. Chem., Int. Ed. Engl.* **1990**, *29*, 279. (c) Spaleck, W.; Antberg, M.; Rohrmann, J.; Winter, A.; Bachmann, B.; Kiprof, P.; Behm, J.; Herrmann, W. *Angew. Chem., Int. Ed. Engl.* **1992**, *31*, 1347−1350. (d) Spaleck, W.; Küber, F.; Winter, A.; Rohrmann, J.; Bachmann, B.; Antberg, M.; Dolle, V.; Paulus, E. *Organometallics* **1994**, *13*, 954. (e) Stehling, U.; Diebold, J.; Kirsten, R.; Röll, W.; Brintzinger, H.-H.; Jüngling, S.; Mülhaupt, R.; Langhauser, F. *Organometallics* **1994**, *13*, 964. (f) Jüngling, S.; Mülhaupt, R.; Stehling, U.; Brintzinger, H. H.; Fischer, D.; Langhauser, F. *J. Polym. Sci.: Part A: Polym. Chem.* **1995**, *33*, 1305.

(3) Resconi, L.; Piemontesi, F.; Camurati, I.; Nifant'ev, I. E.; Ivchenko, P. V.; Kuz'mina, L. G. *J. Am. Chem. Soc.* **1998**, *120*, 2308−2321.

(4) Nifant'ev, I. E.; Ivchenko, P. V. *Organometallics* **1997**, *16*, 713. Nifant'ev, I. E.; Ivchenko, P. V.; Kuz'mina, L. G.; Luzikov, Yu. N.; Sitnikov, A. A.; Sizan, O. E. *Synthesis* **1997**, 469.

10.1021/om990487o CCC: $19.00
Publication on Web 01/20/2000

Chart 1

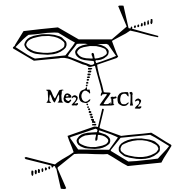

rac-[Me$_2$C(3-*t*-Bu-1-Ind)$_2$]ZrCl$_2$

1

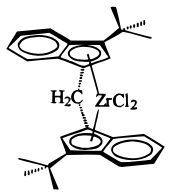

rac-[CH$_2$(3-*t*-Bu-1-Ind)$_2$]ZrCl$_2$

2

(**1**/MAO), producing *i*-PP with no 2,1 units, *mmmm* ≈ 95%, T_m = 152 °C, and $\bar{M}_v \approx 90{,}000$ at T_p = 50 °C, performs far better than the prototypical *rac*-[C_2H_4(1-Ind)$_2$]ZrCl$_2$ or the related *rac*-[Me$_2$C(1-Ind)$_2$]ZrCl$_2$.[3] However, **1**/MAO could not match the performance of the best chiral zirconocenes now being considered for industrial use,[2d−f,5] and the metalation step does not lead to a pure racemic compound (although *meso*-**1** is inactive in propene polymerization). In addition, the synthesis of the 2,2-bis(1-*tert*-butyl-3-indenyl)propane ligand precursor for **1** is not optimal: conversion based on *tert*-butylindene ranges from 50 to 70%, but its isolation is not easy and requires either high-temperature distillation (with partial loss of product) or conversion to its dilithium salt and washing to get rid of starting material and byproducts.

Following our discovery of the interesting polymerization performance of R$_2$C(3-alkylindenyl)$_2$zirconium dichlorides,[3] we have developed a novel synthesis of bis(1-indenyl)methane-based ligands[6] and prepared and evaluated several new members of the class of C_2-symmetric *ansa* zirconocenes of general formula *rac*-CH$_2$(Ind′)$_2$ZrCl$_2$, where Ind′ is a substituted indene.[6] Here, we report the synthesis of bis(1-*tert*-butyl-3-indenyl)methane, *rac*-[CH$_2$(3-*t*-Bu-Ind)$_2$]ZrCl$_2$ (**2**, Chart 1) and *rac*-[CH$_2$(3-*t*-Bu-Ind)$_2$]ZrMe$_2$ (**2-Me$_2$**), and the hafnium (**Hf-2**) and titanium (**Ti-2**) analogues of **2**, a comparison of the molecular structures of **2**, **Hf-2**, and **1**, and the results of our study on their propene polymerization performance, to show how a minor change in catalyst structure, as it is in **2** compared to **1**, can lead to a major improvement in both catalyst accessibility and performance.

Results

1. Catalyst Synthesis. Bis(1-*tert*-butyl-3-indenyl)methane (**2L**) was prepared following the simple protocol developed by us for the condensation between substituted indenes and formaldehyde.[6] *tert*-Butylindene is obtained from indene and *tert*-butylbromide (1:3) under phase transfer conditions (KOH/H_2O)[7] with ca. 80 wt % conversion based on indene. Distillation is necessary to obtain *tert*-butylindene free from indene. Bis(1-*tert*-butyl-3-indenyl)methane is obtained reproducibly in ca. 80% conversion based on *tert*-butylindene (*t*-BuInd:CH_2O, 2:1, catalytic *t*-BuOK in DMF, room temperature, 0.5−2 h), Scheme 2.

Scheme 2

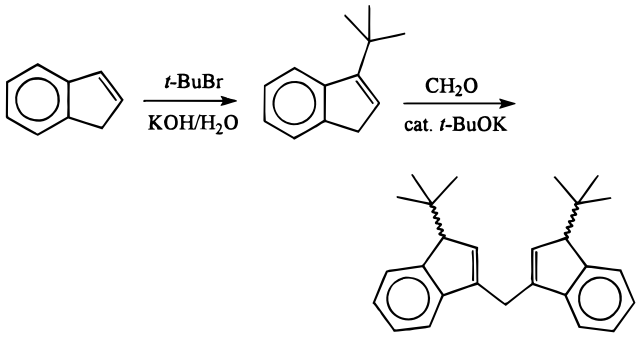

Scheme 3

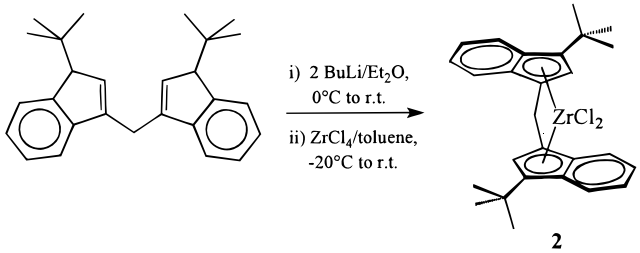

2
pure racemic
66 % yield

Compared to the similar 2,2-bis(1-*tert*-butyl-3-indenyl)propane (**1L**), **2L** is obtained in higher yield under much milder conditions; in addition, **2L** can be obtained as a yellow powder of high chemical purity by simple washing with pentane, while **1L** is a highly viscous oil which requires high-temperature distillation for its isolation. Despite its high steric bulk, **2L** is quantitatively converted into its dilithium salt by reaction with 2 equiv of BuLi in Et$_2$O.

The new *rac*-[CH$_2$(3-*tert*-butyl-1-indenyl)$_2$]ZrCl$_2$ (**2**) was prepared with an easier, higher yield and more stereoselective process compared to the closely related *rac*-[Me$_2$C(3-*tert*-butyl-1-indenyl)$_2$]ZrCl$_2$ (**1**).[3] In fact, chemically and stereoisomerically pure **2** has been prepared with a simple, two-step process, which in addition avoids the use of toxic solvents such as THF and CH_2Cl_2 (Scheme 3).

The racemic configuration of **2** is unambiguously established from the ^{1}H NMR signal of the methylene bridge protons, which is a singlet. In the violet *meso*-**2**, the two diastereotopic methylene bridge protons appear as two doublets.

Following the same route, we have prepared dark red *rac*-[CH$_2$(3-*t*-Bu-1-Ind)$_2$]TiCl$_2$ (**Ti-2**, 14% isolated yield of pure racemate) and orange *rac*-[CH$_2$(3-*t*-Bu-1-Ind)$_2$]-

(5) (a) Spaleck, W.; Antberg, M.; Aulbach, M.; Bachmann, B.; Dolle, V.; Haftka, S.; Küber, F.; Rohrmann, J.; Winter, A. In *Ziegler Catalysts*; Fink, G., Mülhaupt, R., Brintzinger, H. H., Eds.; Springer-Verlag: Berlin, 1995; p 83. (b) Hungenberg, K. D.; Kerth, J.; Langhauser, F.; Marczinke, B.; Schlund, R. In *Ziegler Catalysts*; Fink, G., Mülhaupt, R., Brintzinger, H. H., Eds.; Springer-Verlag: Berlin, 1995; p 363. (c) Bidell, W.; Fischer, D.; Hingmann, R.; Jones, P.; Langhauser, F.; Gregorius, H.; Marczinke, B. In *Proceedings of MetCon '96*; Houston, TX, 1996 (available from the Catalyst Group, P.O. Box 637, Spring House, PA 19477. (d) Ushioda, T.; Fujita, H.; Saito, J. In *Proceeding of the Seventh International Business Forum on Specialty Polyolefins (SPO '97)*; Houston, TX 1997; p 103 (available from Schotland Business Res., Skillman, NJ 08558. (e) Spaleck, W. In *Metallocene-based polyolefins, prepartion, properties and technology*; Scheirs, J., Kaminsky, W., Eds.; Wiley: New York, 1999; p 402. *Ibid*. p 425.

(6) (a) Dang, V. A.; Yu, L.-C.; Balboni, D.; Resconi, L. *Polym. Mater. Sci. Eng.* **1999**, *80*, 469−470. (b) Dang, V. A.; Yu, L.-C.; Balboni, D.; Dall'Occo, T.; Resconi, L.; Mercandelli, P.; Moret, M.; Sironi, A. *Organometallics* **1999**, *18*, 3781.

(7) Dehmlow, E. V.; Bollman, C. *Tetrahedron Lett.* **1991**, *32* (41), 5773.

Scheme 4

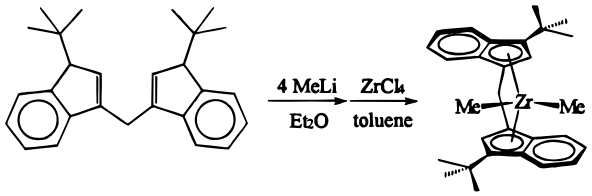

ca. 50 % isolated yield

$HfCl_2$ (**Hf-2**, ca. 54% isolated yield of pure racemate) for comparison purposes. Quite conveniently, **2** can also be prepared in ca. 40% isolated yield from the crude bis-(1-*tert*-butylindenyl)methane ligand as obtained in 80% yield, without further purification, from the reaction between 3-*tert*-butylindene and formaldehyde.

The yellow dimethyl derivative of **2**, *rac*-[CH_2(3-*t*-Bu-1-Ind)$_2$]$ZrMe_2$ (**2-Me$_2$**), can be obtained by conventional methylation of **2** with excess MeMgBr (4 equiv) in ca. 90% yield or through a simpler, one-pot synthesis from the ligand and 4 equiv of MeLi (Scheme 4):[8] this latter method, which is highly efficient and quicker than the conventional one, has the only drawback of producing a lower stereochemical purity, since **2-Me$_2$** is contaminated with 5−10% of its *meso* isomer. However, since *meso*-**2** is inactive toward propene polymerization, this lower stereochemical purity represents only a minor nuisance.

Both **2** and its dimethyl derivative are remarkably soluble in hydrocarbons relative to other *ansa*-metallocenes: **2**, 1.7 g/L in pentane, 50 g/L in toluene; **2-Me$_2$**, 13 g/L in pentane. Solid **2** and **2-Me$_2$** can be stored indefinitely at room temperature, but both are highly sensitive to traces of water in solution.

2. Crystal and Molecular Structures of *rac*-Dichloro[methylenebis(3-*tert*-butyl-η^5-1-indenyl)]-zirconium (2) and *rac*-Dichloro[methylenebis(3-*tert*-butyl-η^5-1-indenyl)]hafnium (Hf-2). The racemic nature of compounds **2** and **Hf-2** has been confirmed by X-ray analysis. Figure 1 shows two different ORTEP views of **2**. Tables 1 (lengths) and 2 (angles) contain the most relevant bonding parameters for the two compounds. Table 3 collects the angles between some relevant least-squares planes, a few slip-fold indicators, and the geometrical parameters described in Chart 2 for compounds **2, Hf-2**, the strictly related isopropylidene-bridged **1**,[3] and the corresponding Zr derivatives lacking the 3-*tert*-butyl substituent, that is, *rac*-[CH_2-(Ind)$_2$]$ZrCl_2$ (**3**) and *rac*-[Me_2C(Ind)$_2$]$ZrCl_2$ (**4**).[6b]

Compound **2** crystallizes in the monoclinic space group $P2_1/c$, while **Hf-2** crystallizes in the orthorhombic space group $P2_12_12_1$ with a solvate toluene molecule. Both compounds show a noncrystallographically imposed C_2 symmetry.

In both compounds the metal atom is pseudotetrahedrally coordinated by the two cyclopentadienyl groups of the bisindenyl moiety and by two chloro ligands. As usual for bent metallocenes, the overall coordination environment is best described by the set of parameters reported in Chart 2, which describe the metal accessibility. In particular, the smaller the "bite angle" β and the bigger the cp−M−cp′ α angle, the more the metal is tucked in the ligand envelope. As can be seen from the values reported in Table 3, the only noticeable difference between parameters for the two zirconium derivatives **2** and **1** consists of a slightly more open angle ϕ (hence a more open angle β) for the methylene-bridged molecule (**2**) with respect to the isopropylidene bridged one (**1**). Moreover, unfavorable steric interactions between the methyl substituents on the *ansa* atom and the aromatic groups leads to a more closed arrangement of the two indenyl moieties (see the bh−cp−cp′−bh′ values in Table 3).

The effects of the presence of the two *tert*-butyl substituents on the metal environment can be envisaged by comparing the pertinent geometrical parameters (Table 3) of **2** versus **3** and **1** versus **4**. As expected from simple steric considerations, β and ϕ increase while δ

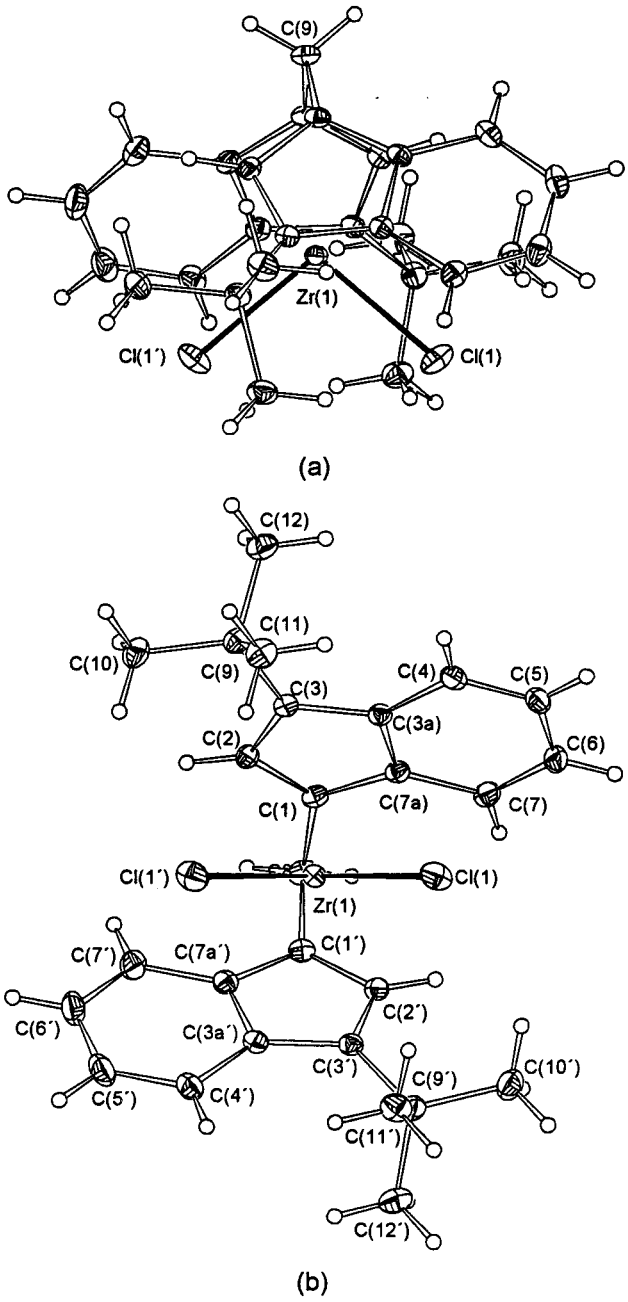

Figure 1. Top (a) and front (b) ORTEP views of **2**. Displacement ellipsoids are drawn at the 30% probability level. Hydrogen atoms are given arbitrary radii.

(8) Our protocol is simpler and more efficient than the one described by Park et al.: Park, J. T.; Woo, B. W.; Yoon, S. C.; Shim, S. C. *J. Organomet. Chem.* **1997**, *535*, 29.

Table 1. Bond Lengths (Å)[a]

	2 (M = Zr)		**Hf-2** (M = Hf)	
	I	II	I	II
M(1)−cp(1)	2.2621(14)	2.2529(14)	2.217(4)	2.219(4)
M(1)−Cl(1)	2.4122(12)	2.4105(11)	2.372(2)	2.386(2)
M(1)−C(1)	2.4450(17)	2.4347(17)	2.418(7)	2.407(7)
M(1)−C(2)	2.4840(17)	2.4750(19)	2.451(7)	2.463(7)
M(1)−C(3)	2.6597(18)	2.6502(18)	2.608(7)	2.606(8)
M(1)−C(3a)	2.694(2)	2.6894(19)	2.644(9)	2.637(7)
M(1)−C(7a)	2.5440(18)	2.5351(17)	2.503(8)	2.510(9)
C(1)−C(2)	1.424(2)	1.416(2)	1.415(10)	1.397(10)
C(1)−C(7a)	1.419(2)	1.423(2	1.415(11)	1.433(12)
C(1)−C(8)	1.515(2)	1.513(2)	1.500(12)	1.504(11)
C(2)−C(3)	1.422(2)	1.417(2)	1.404(11)	1.402(12)
C(3)−C(3a)	1.430(2)	1.432(2)	1.426(11)	1.422(11)
C(3)−C(9)	1.526(2)	1.530(2)	1.535(10)	1.531(10)
C(3a)−C(4)	1.427(2)	1.424(2)	1.449(12)	1.428(13)
C(3a)−C(7a)	1.441(2)	1.445(2)	1.459(12)	1.433(11)
C(4)−C(5)	1.358(3)	1.360(3)	1.378(14)	1.371(13)
C(5)−C(6)	1.413(3)	1.409(3)	1.424(16)	1.384(14)
C(6)−C(7)	1.362(3)	1.355(3)	1.374(15)	1.324(14)
C(7)−C(7a)	1.430(2)	1.423(2)	1.412(11)	1.414(12)
C(9)−C(10)	1.532(2)	1.524(3)	1.553(13)	1.530(15)
C(9)−C(11)	1.539(2)	1.534(2)	1.510(13)	1.524(14)
C(9)−C(12)	1.538(2)	1.538(3)	1.498(13)	1.540(14)

[a] cp refers to the centroid of the five−membered rings of the organic ligand. I and II indicate atoms (I) and primed atoms (II) of **2** and **Hf-2** as shown in Figure 1.

Table 2. Selected Bond Angles (deg)[a]

	2 (M = Zr)		**Hf-2** (M = Hf)	
	I	II	I	II
cp(1)−M(1)−cp(1′)	117.62(3)		118.41(13)	
cp(1)−M(1)−Cl(1)	106.07(2)	106.47(2)	107.44(11)	107.21(11)
cp(1)−M(1)−Cl(1′)	112.52(2)	113.84(2)	112.18(10)	112.60(11)
Cl(1)−M(1)−Cl(1′)	98.82(2)		96.97(9)	
C(2)−C(1)−C(7a)	106.45(13)	106.47(13)	106.4(7)	106.6(7)
C(2)−C(1)−C(8)	126.20(15)	126.13(15)	125.8(8)	126.8(8)
C(7a)−C(1)−C(8)	124.79(15)	125.03(15)	124.8(7)	124.2(7)
C(1)−C(2)−C(3)	110.51(14)	111.11(14)	111.6(7)	111.5(8)
C(2)−C(3)−C(3a)	106.28(14)	106.00(14)	106.2(7)	106.0(7)
C(2)−C(3)−C(9)	126.14(14)	124.96(14)	126.0(7)	125.2(7)
C(3a)−C(3)−C(9)	126.61(15)	127.88(14)	126.3(7)	126.9(8)
C(3)−C(3a)−C(4)	133.08(16)	133.78(16)	133.5(8)	134.3(8)
C(3)−C(3a)−C(7a)	108.13(14)	108.23(14)	107.9(7)	108.8(8)
C(4)−C(3a)−C(7a)	118.77(15)	117.92(15)	118.6(8)	116.9(8)
C(3a)−C(4)−C(5)	118.94(17)	119.37(18)	117.9(9)	118.9(9)
C(4)−C(5)−C(6)	122.52(17)	122.17(18)	122.4(10)	122.4(10)
C(5)−C(6)−C(7)	120.84(17)	121.15(19)	121.3(9)	121.2(10)
C(6)−C(7)−C(7a)	118.93(17)	118.78(18)	118.8(9)	119.6(10)
C(1)−C(7a)−C(3a)	108.60(14)	108.15(14)	107.9(6)	107.2(7)
C(1)−C(7a)−C(7)	131.48(15)	131.37(16)	131.2(8)	132.0(8)
C(3a)−C(7a)−C(7)	119.92(15)	120.48(16)	120.9(8)	120.8(9)
C(1)−C(8)−C(1′)	102.23(12)		102.5(6)	
C(3)−C(9)−C(10)	110.08(14)	110.71(14)	107.1(7)	106.4(9)
C(3)−C(9)−C(11)	111.68(14)	112.12(15)	112.0(7)	113.5(7)
C(3)−C(9)−C(12)	108.26(13)	107.45(14)	111.0(7)	109.2(8)
C(10)−C(9)−C(11)	108.91(15)	108.68(16)	108.6(8)	108.5(9)
C(10)−C(9)−C(12)	108.68(15)	108.38(16)	108.0(8)	109.9(9)
C(11)−C(9)−C(12)	109.18(15)	109.43(15)	110.0(8)	109.3(9)

[a] cp refers to the centroid of the five-membered rings of the organic ligand. I and II indicate atoms (I) and primed atoms (II) of **2** and **Hf-2** as shown in Figure 1.

and γ decrease upon substitution in the 3-position. From the side of the indenyl ligand, we observe a larger slippage Δ and a smaller folding angle Ω in the substituted derivatives (but the latter is probably uninformative given that its value is strongly determined by the out-of-plane displacement of the C(3) atom and cannot be taken as a measure of the "indenyl" folding in the usual way).

Complexes of zirconium and hafnium with the same ligand environment present a very similar geometry and usually possess analogous chemical properties. As expected, the molecular structures of **2** and **Hf-2** are nearly identical, the main difference being the shorter metal−carbon and metal−chlorine bond distances for the hafnium derivative with respect to the zirconium one (mean values 2.525(9) versus 2.561(2) and 2.379(2) versus 2.4114(12) for carbon and chlorine, respectively), in accordance with the lanthanide contraction. As a consequence, the metal atom is less accessible in the hafnium derivative with respect to the zirconium one, as can be judged by the β and α values reported in Table 3. For the very same reasons the out-of-plane bending θ of the *tert*-butyl substituent is larger for the Hf derivative. According to an adaptation by Schlogl[9] of the Cahn−Ingold−Prelog rules, the stereoisomer represented in Figure 1 has an *S*,*S* configuration at C(1) and C(1′), respectively.

Table 3. Relevant Geometrical Parameters[a]

	2	**Hf-2**	**1**	**3**	**4**
α	117.6	118.4	118.3	117.4	118.1
β	76.4	74.2	75.1	72.4	70.9
ϕ	102.2	102.5	100.1	101.4	99.7
δ	82.8	83.5	83.0	84.8	85.0
γ	13.0	14.2	12.5	14.5	14.4
θ	8.5	10.2	9.1		
al−*bz*	2.8	3.2	2.4	2.2	2.4
MCl_2−*cp*	38.3	37.2	37.6	36.2	35.5
bh−cp−cp′−bh′	153.9	152.7	149.6	150.8	149.2
Ω	0.4	1.0	1.1	1.3	1.9
Δ	0.28	0.25	0.27	0.20	0.19

[a] All quantities in degrees, apart from Δ (Å). The angles α, β, γ, δ, and ϕ are defined in Chart 2. θ is the angle between the C(3)−C(9) vector and the ring least-squares plane. *al*, *bz*, *cp*, and MCl_2 refer to the least-squares planes defined by the allylic moiety [C(1), C(2), C(3)], the aromatic six-membered ring, the five-membered ring, and the MCl_2 atoms, respectively. bh refers to the centroid of the bridge-head atoms [C(3a) and C(7a)]. Ω is the angle between the plane defined by the allylic moiety and the least-squares plane defined by the atoms C(1), C(7a), C(3a), and C(3); Δ is the distance between the perpendicular projection of the heavy atom on the ring least-squares plane and the ring centroid.

Chart 2. Schematic Representation of an *ansa*-Metallocene Molecule Detailing the Angles Listed in Table 3[a]

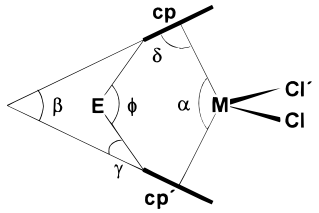

[a] ϕ Is the angle C(1)−C(8)−C(1′); δ is the angle between the M−cp vector and the *cp* least-squares plane; γ is the angle between the C(1)−C(8) vector and the *cp* least-squares plane; β is the angle between the least-squares planes of the two cyclopentadienyl ligands; and α is the angle cp−M−cp′.

3. Propene Polymerization. Comparison with Other Catalysts, Influence of the Al/Zr Ratio, and Catalyst Aging. The racemic, C_2-symmetric **2**, after being activated with methylalumoxane (MAO), is a highly active catalyst for the isospecific polymerization of propene. In the present study, we have used a commercial (Witco) 10% solution of MAO in toluene,

(9) Schlögl, K. *Top. Stereochem.* **1966**, *1*, 39.

Table 4. Summary of Crystal Data, Data Collection, and Structure Refinement Parameters

	2	**Hf-2**
	Crystal Data	
formula	$C_{27}H_{30}Cl_2Zr$	$C_{27}H_{30}Cl_2Hf{\cdot}C_7H_8$
fw	516.63	696.03
cryst syst	monoclinic	orthorhombic
space group	$P2_1/c$ (No. 14)	$P2_12_12_1$ (No. 19)
a (Å)	10.240(5)	11.015(2)
b (Å)	9.439(5)	14.353(4)
c (Å)	24.688(12)	19.226(4)
β (deg)	93.86(1)	
V (Å^3)	2381(2)	3039.6(12)
Z	4	4
F(000)	1064	1392
density (g cm^{-3})	1.441	1.521
abs coeff (mm^{-1})	0.698	3.628
cryst description	purple plate	orange prism
cryst size (mm)	0.45 × 0.23 × 0.10	0.20 × 0.12 × 0.10
	Data Collection	
diffractometer	Siemens SMART	Enraf-Nonius CAD-4
scan mode	ω	ω
θ range (deg)	$1.6 \le \theta \le 27.2$	$3.0 \le \theta \le 25.0$
index ranges	$-12 \le h \le 13$	$0 \le h \le 13$
	$-12 \le k \le 11$	$0 \le k \le 16$
	$-31 \le l \le 31$	$-22 \le l \le 22$
intensity decay (%)	none	12
abs corr	SADABS	ψ scan
transmn factors (min, max)	0.765, 0.934	0.549, 0.714
no. of measd reflns	22523	5835
no. of indep reflns	4873	5326
R_{int}, R_σ[a]	0.0216, 0.0204	0.0320, 0.0401
no. of reflns with $I > 2\sigma(I)$	4279	4417
	Refinement	
no. of data/restraints/params	4873/0/271	4417/0/271
weights (a, b)[b]	0.032, 0.25	0.052, 2.44
goodness-of-fit $S(F^2)$[c]	1.025	1.046
$R(F)$, $I > 2\sigma(I)$[d]	0.0216	0.0309
$wR(F^2)$, all data[e]	0.0567	0.0800
largest diff peak and hole (e Å^{-3})	0.286, −0.364	0.632, −0.434

[a] $R_{int} = \sum|F_o^2 - F_{mean}^2|/\sum|F_o^2|$; $R_\sigma = \sum|\sigma(F_o^2)|/\sum|F_o^2|$. [b] $w = 1/[\sigma^2(F_o^2) + (aP)^2 + bP]$, where $P = (F_o^2 + 2F_c^2)/3$. [c] $S = [\sum w(F_o^2 - F_c^2)^2/(n-p)]^{1/2}$, where n is the number of reflections and p is the number of refined parameters. [d] $R(F) = \sum||F_o| - |F_c||/\sum|F_o|$. [e] $wR(F^2) = [\sum w(F_o^2 - F_c^2)^2/\sum wF_o^4]^{1/2}$.

which contains about 20−30% $AlMe_3$. The solution was further diluted to 5% in toluene. In all polymerization experiments, Al(*i*-Bu)$_3$ (0.5 mmol/L) was used to scavenge possible impurities in the monomer. The polymerization results are compared in Table 5 with those from **1**/MAO[3] and two of the best isospecific zirconocenes being considered for industrial use, that is, Targor's *rac*-Me_2Si(2-Me-4-Ph-Ind)$_2ZrCl_2$/MAO[2d,5a] and Chisso's *rac*-Me_2Si(2,3,5-Me_3-Cp)$_2ZrCl_2$/MAO.[2a,5d] In analogy with the behavior of **1**/MAO,[3] **2**/MAO is fully regiospecific: no 2,1 or 3,1 propene units could be detected in the ^{13}C NMR spectra of *i*-PP samples. It is apparent that **2**/MAO has a better performance, in terms of *i*-PP properties (molecular weight and isotacticity), than **1**/MAO. In addition, **2**/MAO produces *i*-PP with melting point and molecular weight similar to those of *i*-PP from *rac*-Me_2Si(2,3,5-Me_3-Cp)$_2ZrCl_2$.[5d] *rac*-Me_2Si(2-Me-4-Ph-Ind)$_2ZrCl_2$ remains the chiral zirconocene with the highest performance, in terms of activity and *i*-PP stereoregularity and molecular weight,[2d,5a] but has a lower regiospecificity.[10] The balance between stereo- and regioregularity results in a melting point of *i*-PP that is close to that of *i*-PP produced with the less stereospecific but much more regiospecific catalyst **2**. The ultimate catalyst's evaluation, in terms of the cost/performance balance, will have to be carried out on the supported zirconocene/MAO systems, at much lower (50−500) Al/Zr ratios, a study currently ongoing in our laboratories. In any case, **2** is among the simplest and most readily prepared chiral *ansa*-zirconocenes available to date.

The inactivity of **Ti-2**, to be expected at these relatively high temperatures because of reduction, might also be due to the smaller ionic radii of titanocenes versus zirconocenes. Also the almost nil activity of **Hf-2** could be attributed to the lower accessibility of the metal, although it could also be ascribed to the higher stability of the Hf−C bond with respect to the Zr−C bond.[11] It is generally observed that hafnocenes are much less active than zirconocenes in propene polymerization, although exceptions have been reported.[12]

As expected, by increasing catalyst loading, the activity increases (compare entries 1 and 2 in Table 6). As commonly observed with zirconocene catalysts, **2** shows a strong dependence of catalyst activity on the Al_{MAO}/Zr molar ratio (T_p = 60 °C). The polymerization results and the available polymer characterization are shown in Table 6. By looking at the trend of activity versus Al_{MAO}/Zr ratio, it is clear that we have not reached maximum catalyst activity for **2**/MAO. Although working with very high Al_{MAO}/Zr ratios (>1000 mol/mol) seems unrealistic in view of the requirements and limitations of the available catalyst supportation techniques, estimating the maximum activity of a zirconocene catalyst is important for catalyst development, as the *maximum activity represents the intrinsic Zr activity* at a given set of T_p and monomer concentration conditions, hence the target for supportation and activation studies. A catalyst activity of more than 120 kg_{PP}/($mmol_{Zr}$ h) (that is, 240 kg_{PP}/(g_{cat} h)) at an Al_{MAO}/Zr ratio of 8000 is quite significant.

The Al/Zr ratio does not seem to have a relevant effect on *i*-PP properties: melting points (T_m = 156−161 °C) and molecular weights are relatively unaffected by this variable in the range investigated.

Catalyst (**2** + MAO in toluene) aging seems to have a limited influence (if any) on activity: in one test, ca. 20% deactivation has been observed after 30 h, although this might be due to manipulation rather than chemical deactivation.

We have seen above that the activity of **2**/MAO is strongly and adversely affected by the lowering of the Al/Zr ratio. Our working hypothesis was that at lower Al/Zr ratios fewer active Zr centers would be formed due to incomplete Zr alkylation, with the specific catalyst activity remaining the same. This is one of the reasons for investigating the polymerization behavior of *rac*-[CH_2(3-*t*-Bu-1-Ind)$_2$]$ZrMe_2$/MAO (**2-Me$_2$**/MAO).

(10) In our hands, *rac*-Me_2Si(2-Me-4-Ph-Ind)$_2ZrCl_2$ gave, at 70 °C in liquid propene (Al_{MAO}/Zr = 10 000), with an activity close to that of ref 2d, an *i*-PP with M_v = 734 000, *mmmm* = 99.55%, and 2,1 = 0.46%. Unpublished results from our laboratory.

(11) Schock, L. E.; Marks, T. J. *J. Am. Chem. Soc.* **1988**, *110*, 7701.

(12) Ewen, J. A.; Haspeslagh, L.; Atwood, J. L.; Zhang, H. *J. Am. Chem. Soc.* **1987**, *109*, 6544. Resconi, L.; Piemontesi, F.; Franciscono, G.; Abis, L.; Fiorani, T. *J. Am. Chem. Soc.* **1992**, *114*, 1025.

Table 5. Propene Polymerization with 2/MAO: Comparison with Reference Metallocene Catalysts[a]

catalyst	T_p, °C	Al_{MAO}/Zr, molar	activity, $kg_{PP}/(mmol_{Zr}\ h)$	$\bar{M}_v$[b]	$\bar{M}_w$[c]	$\bar{M}_w/\bar{M}_n$	$T_{m(II)}$, °C	*mmmm*,[d] %	2,1,[d] %
1[e]	50	8000	124.6	88 700	111 400	2.0	152	94.8	0
2	50	1000	37.4	195 700	236 800	2.8	162	97.0	0
2	60	8000	123.4	91 100	127 000	2.1	161	96.8	0
rac-Me$_2$Si(2,3,5-Me$_3$Cp)$_2$ZrCl$_2$[f]	50	15 000	207		184 500	1.9	161	96.4	0.3
rac-Me$_2$Si(2-Me-4-Ph-Ind)$_2$ZrCl$_2$[g]	70	15 000	755		729 000		157	95.2	0.5[h]

[a] Experimental conditions: 4.25 L stainless steel reactor; liquid propene, 2 L; cocatalyst MAO Witco, 5% in toluene; 1 h, 1 mmol Al(*i*-Bu)$_3$ added to the monomer. [b] Calculated from the experimental intrinsic viscosities ($[\eta]_{THN,\ 135\ °C}$) according to the $[\eta] = K(\bar{M}_v)^\alpha$ with $K = 1.93 \times 10^{-4}$ and $\alpha = 0.74$. [c] From SEC, *o*-DCB, 135 °C. [d] From ^{13}C NMR. The values are referenced to the total methyl signals. [e] Data from ref 3. [f] Data from ref 5d. [g] Data from ref 2d. [h] Data from our laboratory, see ref 10.

Table 6. Propene Polymerization with 2/MAO: Influence of Al/Zr Ratio, Aging, Metal, and *σ*-Ligand[a]

run no.	catalyst	mg	Al_{MAO}/Zr, molar	aging	activity, $kg_{PP}/(mmol_{Zr}\ h)$	M_v,[b] g/mol	$T_{m(II)}$, °C	ΔH, J/g	*mmmm*,[d] %
1	**2**	4	200	10 min	15.5	112 000	157	113	96.5
2	**2**	2	300	10 min	4.1	108 900	157	110	
3	**2**	2	500	6 h	32.0	114 611	159	109	
4	**2**	2	500	30 h	24.5	106 000	156	109	
5	**2**	2	1000	10 min	45.6	108 900	156	109	96.5
6	**2**	1.5	3000	10 min	71.8	82 600	159	113	
7	**2**	1	8000	10 min	123.4	91 000	161	104	96.8
8	**Ti-2**	2	3000	10 min	none				
9	**Hf-2**	4	1000	10 min	0.1				
10	**2-Me$_2$**	4	200	10 min	23.8	112 000	157	112	97.0
11	**2-Me$_2$**	4	200[e]	10 min	35.7	134 000			

[a] Experimental conditions: 4.25 L stainless steel reactor; liquid propene, 2 L; cocatalyst MAO Witco, 5% in toluene; 60 °C, 1 h, 1 mmol Al(*i*-Bu)$_3$ added to the monomer. [b] Calculated from the experimental intrinsic viscosities ($[\eta]_{THN,\ 135\ °C}$) according to the $[\eta] = K(M_v)^\alpha$ with $K = 1.93 \times 10^{-4}$ and $\alpha = 0.74$. [c] *o*-DCB, 135 °C. [d] Primary monomer insertion errors from ^{13}C NMR, 400 MHz. No secondary units can be detected by ^{13}C NMR. [e] Dried MAO (60 °C, 6 h, 1 mmHg).

Table 7. Propene Polymerization with 2/MAO: Influence of the Polymerization Temperature[a]

sample no.	**2**, mg	T_p, °C	activity, $kg_{PP}/(mmol_{Zr}\ h)$	$\bar{M}_v$,[b] g/mol	$\bar{M}_w$[c]	$\bar{M}_w/\bar{M}_n$	$T_{m(II)}$, °C	ΔH, J/g	*mmmm*,[d] %	*b*[d]
12	1.5	70	47.8	76 100	74 100	3.1	154	112	95.2	0.9903
5	2	60	45.6	108 900	133 800	2.7	156	109	96.5	0.9928
13	2	50	37.4	195 700	236 800	2.8	162	108	97.0	0.9939
14	2	40	27.3	326 200	390 000	2.9	160	105	97.3	0.9945
15	2	30	16.7	662 600	785 700	3.0	163	106	97.8	0.9955

[a] Experimental conditions: liquid monomer, cocatalyst MAO Witco, 5% in toluene; Al/Zr = 1000; 1 h. [b] Calculated from the experimental intrinsic viscosities ($[\eta]_{THN,\ 135\ °C}$) according to the $[\eta] = K(\bar{M}_v)^\alpha$ with $K = 1.93 \times 10^{-4}$ and $\alpha = 0.74$. [c] $C_6H_3Cl_3$, 135 °C. [d] Determined by ^{13}C NMR assuming the enantiomorphic site model, on the homogenized samples. No secondary units can be detected.

By using 2-Me$_2$/MAO under the same conditions, the activity is increased to 23.8 kg/(mmol$_{Zr}$ h). The *i*-PP made by both **2**/MAO and **2-Me$_2$**/MAO under the present conditions has a viscosity average molecular weight around 105 000, T_m around 157 °C, and practically no extractables. The MAO used was the commercial Witco 10% solution in toluene, a product that contains about 30% of total Al as unreacted AlMe$_3$ (TMA). The presence of TMA was found in the past to lower catalyst activity. In our case, at these low Al/Zr ratios, we expected TMA to be even more detrimental to activity, so we tested 2-Me$_2$ in combination with dried MAO (volatiles were removed from a Witco commercial toluene gel containing 30% MAO, and the glassy residue was further dried at 60 °C, 1 mmHg for 6 h). In this case, activity was observed to increase to 35.7 kg/(mmol$_{Zr}$ h). At the same time, the molecular weight is slightly increased to 134 000.

Influence of the Polymerization Temperature. The influence of polymerization temperature on catalyst activity and polymer properties has been evaluated in liquid monomer in the range 30−70 °C, at Al/Zr = 1000.

The polymerization results and the molecular characterization of *i*-PP (on the powder as recovered from the reactor) are shown in Table 7. To obtain more reliable data, the polymer samples were extruded in the grader, and the microstructural data obtained on the extruded strand are also reported in Table 7. The activities (as *A*/[M], activities normalized against propene concentration) versus T_p show a linear dependence. Such a plot should *not* give a linear dependence, but an exponential behavior. The apparent linearity of the activity/temperature dependence suggests partial catalyst decay at the higher temperatures. The viscosity average molecular weights obtained in the temperature interval 30−70 °C with **2**/MAO are consistently higher than those previously obtained with the **1**/MAO catalyst. Number average degrees of polymerization ($\bar{P}_n$) can be estimated from the viscosity numbers in the assumption that $\bar{M}_v \approx \bar{M}_w$ and $\bar{M}_w/\bar{M}_n = 2$.

For single-center catalysts, this assumption is reasonable, since, from SEC data (see Table 6), for **2** we found $2.1 < \bar{M}_w/\bar{M}_n < 3.1$ and $1.3 \times \bar{M}_w < \bar{M}_{v,[\eta]} < 1.4 \times \bar{M}_w$.

The validity of the average viscosity molecular weight data can be assessed from the $\ln(\bar{P}_n)$ versus $1/T_p$ plot, which must give a linear correlation. If linear, from the slope of this Arrhenius plot one obtains the overall difference in activation energy between propene insertion and chain transfer ($\Delta\Delta E^\ddagger_{tr}$). In other words, the $\Delta\Delta E^\ddagger$ value is a measurement of how much the molec-

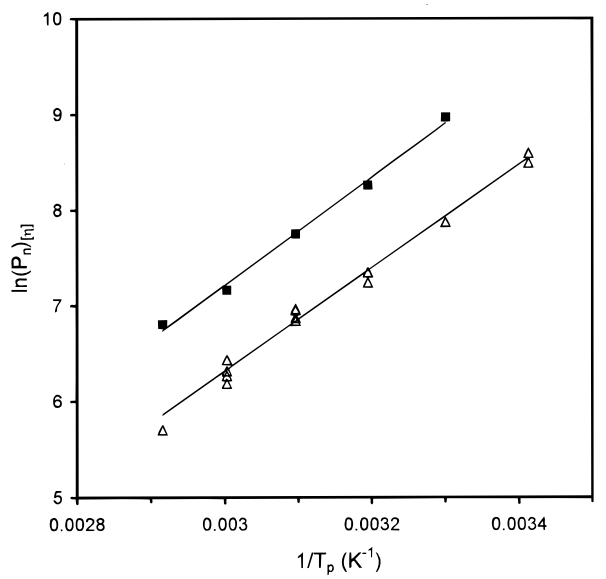

Figure 2. Arrhenius plots of $\ln(\bar{P}_n)$ versus $1/T_p$: (■) **2**/MAO, $\Delta\Delta E^{\ddagger} = 11.2 \pm 0.5$ kcal/mol, $R = 0.997$; (△) **1**/MAO, $\Delta\Delta E^{\ddagger} = 10.7 \pm 0.4$ kcal/mol, $R = 0.992$. $\bar{P}_n$ is the number average degree of polymerization estimated from average viscosity molecular weights, assuming $\bar{M}_v = \bar{M}_w$ and $\bar{M}_w/\bar{M}_n = 2$.

ular weight of *i*-PP changes by changing the polymerization temperature. The $\ln(\bar{P}_n)$ from viscosity measurements versus $1/T_p$ plots for *i*-PP from **2**/MAO and **1**/MAO are shown in Figure 2. The $\Delta\Delta E^{\ddagger}$ values obtained for both catalysts are among the highest so far observed for zirconocene catalysts and indicate that the most effective tool for molecular weight variation is the polymerization temperature (small changes in T_p cause large changes in the molecular weight of *i*-PP). The close $\Delta\Delta E^{\ddagger}_{tr}$ values from [η] (11.2 ± 0.5 kcal/mol) and from SEC (12.0 ± 0.6 kcal/mol) for **2** confirm the reliability of the molecular weight data.

The isotacticity of the samples was measured on the extruded strands, as percent *mmmm* by ^{13}C NMR, and again *i*-PP samples from **2**/MAO are more isotactic than those from **1**/MAO: this higher stereoregularity is reflected in the higher melting points, among the highest reported for chiral zirconocenes.

The samples, produced with a stereochemically pure, single-center catalyst, should not have extractables, that is, fraction of material soluble in xylene at room temperature. In practice, xylene solubles are around 0.2−0.4 wt %, values that are close to the detection limit of the method, and no detectable oligomers (fraction soluble in acetone).

From the pentad content one can evaluate the probability of correct monomer insertion, *b*, which defines the catalyst stereospecificity *at a given* T_p. From the slope of the Arrhenius plot $\ln[b/(1-b)]$ versus $1/T_p$, if linear, the value of enantioface selectivity ($\Delta\Delta E^{\ddagger}_{enant}$) is then obtained. This value quantifies the change of catalyst stereospecificity with T_p. The Arrhenius plots for the two catalysts (**2**/MAO, $\Delta\Delta E^{\ddagger}_{enant} = 3.7 \pm 0.4$; **1**/MAO, $\Delta\Delta E^{\ddagger}_{enant} = 4.5 \pm 0.4$) show that **2** and **1** have similar stereospecificity. Since the difference in stereocontrol resides in the preexponential factor, we assume that the molecular structure of the active species generated from **2** is more rigid than that in **1**.

Conclusions

We have described the synthesis and performance of *rac*-[CH_2(3-*tert*-butyl-1-indenyl)]$_2ZrCl_2$ (**2**) and its dimethyl derivative, *rac*-[CH_2(3-*tert*-butyl-1-indenyl)]$_2ZrMe_2$ (**2-Me$_2$**), in the polymerization of propene under homogeneous (unsupported) conditions. MAO-activated **2** produces *i*-PP with good activities (e.g., 45 $kg_{PP}/(mmol_{Zr}$ h) at 60 °C in liquid monomer and Al/Zr of 1000 mol/mol), average viscosity molecular weights from 76 000 (T_p = 70 °C) to 660 000 (T_p = 30 °C), and melting points from T_m = 154 °C (T_p = 70 °C) to T_m = 163 °C (T_p = 30 °C). Isotacticities of *i*-PP from **2**/MAO, ranging from 95% pentad content (70 °C, bulk) to 97% (40 °C, bulk), are notably higher than those obtained with our previous catalyst, *rac*-[Me_2C(3-*tert*-butyl-1-indenyl)]$_2ZrCl_2$ (**1**). **2** shows a marked improvement with respect to its closest analogue **1** also in terms of molecular weights and, obviously, melting points (**1**/MAO, $\bar{M}_v \approx 89\,000$ and T_m = 152 °C at 50 °C and $\bar{M}_v \approx 24\,000$ and T_m = 140 °C at 70 °C under the same conditions). **2-Me$_2$**/MAO, at the quite low Al_{MAO}/Zr ratio of 200, is appreciably more active than **2**/MAO and produces *i*-PP with the same molecular characteristics.

The degree of isotacticity of *i*-PP from **2/MAO** and **2-Me$_2$**/MAO is similar to those of the xylene-insoluble fractions of *i*-PP from heterogeneous Ti−$MgCl_2$ catalysts.[13] With **2**, however, the xylene-soluble (amorphous) fraction is well below 1 wt % (xylene solubles at room temperature = 0.3−0.5 wt %, oligomers below detectability), compared to 1−10 wt % typical of *i*-PP from heterogeneous Ti−$MgCl_2$ catalysts. Melting points are generally lower than those of *i*-PP from Ti catalysts, but close to or higher than those reported for the most stereospecific zirconocene catalysts. Molecular weight distributions are narrow ($\bar{M}_w/\bar{M}_n$ = 2−3), as typical of metallocene catalysts.

We see **2** as an isospecific zirconocene catalyst with a very good cost/performance balance and, far from representing a replacement for industrial heterogeneous Ti−$MgCl_2$ catalysts, as a complement to the same. **2**/MAO is suitable for the production of *i*-PP homopolymer with medium-high melt flow rates, narrow molecular weight distribution, and very low extractable (oligomer) content. The substantial improvement in catalyst performance observed on going from **1** to **2**, achieved with the quite small structural change in the bridge, suggests that additional small variation of the ligand structure within the class of our single-C-bridged, 3-R-substituted, bisindenyl-based, C_2-symmetric *ansa*-zirconocenes might further improve catalyst activity and *i*-PP molecular weights. The influence of hydrogen, propene concentration, and comonomers has been investigated and will be reported in the future.

Experimental Section

General Procedures. All operations were performed under nitrogen by using conventional Schlenk-line techniques. Solvents were purified by degassing with N_2 and passing over activated (8 h, N_2 purge, 300 °C) Al_2O_3 and stored under

(13) Chadwick, J. C.; Morini, G.; Balbontin, G.; Sudmeijer, O. *Macromol. Chem. Phys.* **1998**, *199*, 1873.

nitrogen.[14] MeLi (Acros), BuLi, MeMgCl (Aldrich), indene (Aldrich, technical, 92% by GC), *tert*-butyl bromide (Aldrich, 98%), Adogen (Aldrich), KOH (Carlo Erba, 85%), DMF (Merck, 99.7%), formaldehyde (Aldrich, 37 wt % in water), and *t*-BuOK (Fluka, 97%) were used as received. All compounds were analyzed by ^{1}H NMR on a DPX 200 Bruker spectrometer operating at 200.13 MHz ($CDCl_3$, referenced against the peak of residual $CHCl_3$ at 7.25 ppm; CD_2Cl_2, referenced against the peak of residual $CHDCl_2$ at 5.35 ppm; C_6D_6, referenced against the peak of residual C_6D_5H at 7.15 ppm). All NMR solvents were dried over CaH_2 or P_2O_5 and distilled before use. Preparation of the samples was carried out under nitrogen using standard inert atmosphere techniques. Due to the low solubility of some zirconocenes, these samples were prepared as saturated solutions in 0.5 mL of solvent in a 5 mm NMR tube. The metallocenes gave satisfactory elemental analysis.

Polymer Analysis. The ^{13}C NMR analyses of *i*-PP samples were performed on a Bruker DPX 400 in $C_2D_2Cl_4$ at 130 °C as previously described.[15] The polymer molecular weights were determined by viscosimetry (intrinsic viscosity [η], in THN at 135 °C) and, on selected samples, by size exclusion chromatography on a Waters 150 at 135 °C in *o*-DCB. The *i*-PP melting points and heats of fusion reported are those obtained in the second melt, heating rate 20 °C/min, on a DSC Mettler.

Synthesis of *tert*-Butylindene (slightly modified from ref 7). Aqueous KOH, indene (technical grade, 92% by GC), and a solution of Adogen (MW 464) and *tert*-butyl bromide (MW 137.03) were introduced in this order, at either room temperature or 50 °C, in a 2 L jacketed glass reactor (Büchi), connected to a thermostat, and equipped with a mechanical stirrer (800 rpm) and thermocouple, previously purged with nitrogen. The organic phase turned green. The mixture was heated to 60 °C and vigorously stirred for 2 h (a pressure buildup is observed) and then cooled to room temperature.

The organic phase was extracted with technical hexane (3 × 200 mL), filtered over $MgSO_4$, and analyzed by GC (conversion ca. 75−85 wt %). The solution was evaporated under reduced pressure, and the resulting dark brown viscous liquid was distilled at 13 mmHg, collecting the fraction boiling between 100 and 107 °C (isolated yields 60−70%, GC purity 98−99%). The ^{1}H NMR analysis showed the presence of both 3-*tert*-butylindene (80%, ^{1}H NMR ($CDCl_3$, δ, ppm): 1.55, *t*-Bu, s, 9H; 3.42, CH_2, d, J = 2.08, 2H; 6.34, CH, t, J = 2.08; 7.24−7.81, Ar, 4H) and 1-*tert*-butylindene (20%, ^{1}H NMR ($CDCl_3$, δ, ppm): 1.19, *t*-Bu, s, 9H; 2.29, CH, m, 1H; 6.67, CH, dd, J = 1.86, 0.62; 6.95, CH, dd, J = 1.86, 0.62; 7.24−7.81, Ar, 4H).

Synthesis of Bis(1-*tert*-butyl-3-indenyl)methane. In a three-neck, 1 L flask with stirring bar were introduced in this order 10.32 g of *t*-BuOK (92 mmol) dissolved in 400 mL of DMF and 80.6 g of *tert*-butylindene (98.2% by GC, 460 mmol). A 18.6 mL sample of aqueous formalin (37 wt %, 6.9 g, 230 mmol) was added dropwise over 15 min. During the addition, bubbling was not observed, while complete mixing required about 30 min. A mildly exothermic reaction was observed, and the solution turned red and finally dark red. The mixture was stirred at room temperature for 2 h from the end of the addition and then quenched by pouring the mixture on ice and NH_4Cl, extracted with Et_2O (2 × 250 mL), and concentrated under reduced pressure to yield an oily orange product, which crystallized upon standing (ca. 1 h). Final after extraction: 1-*t*-BuInd, 0.3%; 3-*t*-BuInd, 2.8%; target product (M^+ 356), 78.3%; M^+ 540, 8.9%. Yield of raw product: 83.6 g, corresponding to a yield of 79.9%. This product was washed with pentane: the pentane extract (67.7 g) contained 66.3 wt % of the target product; the residue from pentane (14.5 g of light yellow powder) was pure bis(1-*tert*-butyl-3-indenyl)methane (99.8 wt % by GC). ^{1}H NMR ($CDCl_3$, δ, ppm): 1, s, 18H; 3.2, s, 2H; 3.8, s, 2H; 6.2, s, 2H; 7.1−7.7, m, 8H.

When the same reaction was carried out at 50 °C, only the isomerized product was obtained in over 80% yield:

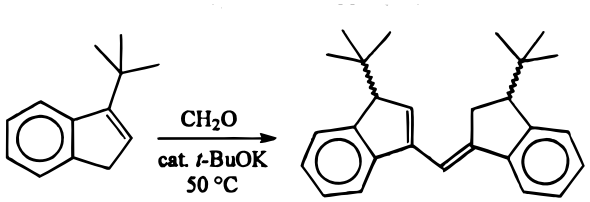

^{1}H NMR ($CDCl_3$, δ, ppm): 0.9, s, 9H; 1.09, s, 9H; 1.3−1.6, m, 1H; 2.8−3.5, m, 3H; 6.6, s, 1H; 6.9, s, 1H; 7.1−8.7, m, 8H.

Synthesis of 2. A 3.46 g sample of bis(3-*tert*-butyl-1-indenyl)methane (98.9% GC, 9.6 mmol) was dissolved in 60 mL of Et_2O in a 250 mL Schlenk tube, and the solution cooled to 0 °C. A 8.8 mL sample of 2.5 M BuLi in hexane (22.0 mmol) was added dropwise over 6 min with stirring. The solution was allowed to warm to room temperature and stirred for 24 h. An increasing turbidity developed with final formation of an orange precipitate. A 2.46 g sample of $ZrCl_4$ (10.6 mmol) was slurried in 60 mL of toluene. The two mixtures were both cooled to −20 °C, and the $ZrCl_4$ slurry in toluene was quickly added to the Li salt suspension in Et_2O; instantly the slurry changed from orange to red. The cooling bath was kept at −20 ± 1 °C for 25 min, then at −17 ± 1 °C for 20 min; then the solution was allowed to warm to 0 °C, and after 20 min the cooling bath was removed. The reaction mixture was stirred overnight at room temperature, and then Et_2O was removed under reduced pressure: the toluene suspension was filtered. The filtrate was evaporated to dryness under reduced pressure to give 3.26 g of a red powder.^{1}H NMR shows the presence of pure **2** (65.7% yield). The residue on the frit (red violet solid) was dried and shown by ^{1}H NMR to contain *meso*:*rac* = 93:7. This was washed with tetrahydrofuran and dried again. The final product (1.2 g of red violet powder) was pure *meso*-**2** (24.2% yield). During the washing with tetrahydrofuran of the residue on the frit a partial isomerization from *meso* to *rac* was noticed, with partial decomposition. This synthesis showed the high solubility of **2** in toluene, about 50 g/L. A similar experiment carried out at room temperature gave pure **2** in 56% yield. Red crystals of **2**, suitable for X-ray analysis, were grown from a concentrated toluene solution at −20 °C.

***rac*-2**: ^{1}H NMR (CD_2Cl_2, δ, ppm) 1.37, *t*-Bu, s, 18H; 4.79, CH_2 bridge, s, 2H; 5.78, Cp-H, s, 2H; 7.08, t, Ar, 2H; 7.34, t, Ar, 2H; 7.49, d, Ar, 2H; 7.76, d, Ar, 2H.

***meso*-2**: ^{1}H NMR (CD_2Cl_2, δ, ppm) 1.48, *t*-Bu, s, 18H; 4.77, CH_2 bridge, d, J = 14.09, 1H; 5.09, CH_2 bridge, d, 1H, J = 14.09; 5.86, Cp-H, s, 2H; 6.87, t, Ar, 2H; 7.09, t, Ar, 2H; 7.63, d, Ar, 2H; 7.70, d, Ar, 2H.

Anal. Calcd for $C_{27}H_{30}Cl_2Zr$: C, 62.8; H, 5.8; Zr, 17.7. Found: C, 60.1; H, 5.8; Zr, 18.2 (Hf, n.d.).

Synthesis of 2-Me$_2$. All operations were performed in the dark, by covering the glassware with aluminum foil. A 7.13 g sample of bis(3-*tert*-butyl-1-indenyl)methane (98.9% GC, 19.8 mmol) was dissolved in 110 mL of Et_2O in a 250 mL dark Schlenk tube, and the solution cooled to 0 °C. A 50.1 mL portion of 1.6 M MeLi in Et_2O (80.2 mmol) was added dropwise over 30 min with stirring.

The reaction mixture was allowed to warm to room temperature and stirred for 24 h. After about 2 h, the lithium salt began to precipitate with final formation of a yellow suspension. A 5.10 g sample of $ZrCl_4$ (21.9 mmol) was slurried in 90 mL of toluene. The two mixtures were both cooled to −30 °C, and the $ZrCl_4$ slurry in toluene was quickly added to the Li salt suspension in Et_2O. The cooling bath was kept at −30 ± 1 °C for 20 min, then at 0 °C for 30 min, and then it was removed. The reaction mixture was stirred overnight at room temperature with final formation of a brown dark suspension.

(14) Pangborn, A. B.; Giardello, M. A.; Grubbs, R. H.; Rosen, R. K.; Timmers, F. J. *Organometallics* **1996**, *15*, 1518.

(15) Resconi, L.; Fait, A.; Piemontesi, F.; Colonnesi, M.; Rychlicki, H.; Zeigler, R. *Macromolecules* **1995**, *28*, 6667.

Et_2O was removed under reduced pressure, and the toluene suspension was filtered. The residue on the frit was dried to give a brown solid and shown by ^1H NMR to contain *meso:rac* = 90:10 and traces of monomethyl compound.

The filtrate was evaporated to dryness under reduced pressure to give 7.0 g of brown powder which contains *rac:meso* = 92:8 (yield 74.2%). A part of this product was further purified by Soxhlet extraction with refluxing pentane (12 h): the extract was a yellow powder which analyzes (^1H NMR) as **2-Me$_2$** contaminated by about 4% of its *meso* isomer.

rac-**2-Me$_2$**: ^1H NMR (C_6D_6, δ, ppm) s, −0.81, 6H, CH_3; s, 1.38, 18H, *t*-Bu; s, 3.84, 2H, CH_2 bridge; s, 5.49, 2H, Cp−H; 6.78, t, Ar, 2H; 6.95, d, Ar, 2H; 7.11, t, Ar, 2H; 7.73, d, Ar, 2H.

meso-**2-Me$_2$**: ^1H NMR (C_6D_6, δ, ppm) s, −1.88, 3H, CH_3; s, 0.36, 3H, CH_3; s, 1.45, 18H, *t*-Bu; d, 3.69, J = 13.94, 1H, CH_2 bridge; d, 4.07, J = 13.94, 1H, CH_2 bridge; s, 5.42, 2H, Cp−H; 6.68, t, Ar, 2H; 6.90, t, Ar, 2H; 7.05, d, Ar, 2H; 7.69, d, Ar, 2H.

Synthesis of 2-Me$_2$ from 2 and MeMgCl. A 15.61 g sample of **2** (30.2 mmol) was dissolved in 200 mL of toluene in a 250 mL Schlenk tube, and the solution cooled to 0 °C. A 22.5 mL portion of 3 M MeMgCl in THF (Fluka, 67.5 mmol) was slowly added with stirring. The solution was allowed to warm to room temperature and stirred for 3.5 h. The resulting red-orange suspension, analyzed by ^1H NMR (C_6D_6), showed the presence of 17% **2-MeCl** and ca. 20% of starting material. Hence, an additional 18 mL of 3 M MeMgCl in THF (54 mmol) was slowly added with stirring at room temperature. The mixture was allowed to stir overnight, yielding a yellow-orange suspension, which contained pure **2-Me$_2$**. The suspension was filtered, and the filtrate was brought to dryness (19 g, contains $MgCl_2(THF)_x$), suspended in 200 mL of pentane, and transferred into a frit with sidearm for continuous extraction. Six hours of extraction with refluxing pentane yielded 13.02 g of yellow solid, which analyzed as pure racemic **2-Me$_2$**. Isolated yield: 91%.

Synthesis of *rac*-[CH$_2$(3-*t*-BuInd)$_2$]TiCl$_2$ (Ti-2). A 6.1 g sample of bis(1-*tert*-butyl-3-indenyl)methane (93.6% by GC, 16.0 mmol) was dissolved in 120 mL of Et_2O in a 250 mL Schlenk tube, and the solution cooled to −20 °C. A 14.4 mL portion of 2.5 M BuLi in hexane (36.0 mmol) was added dropwise over 10 min with stirring. The solution was allowed to warm to room temperature and stirred for 5 h. An increasing turbidity developed with final formation of an orange suspension. A 1.88 mL sample of $TiCl_4$ (17.0 mmol) was dissolved in 120 mL of pentane. The two mixtures were both cooled to −80 °C, and the Li salt suspension in Et_2O was quickly added to the $TiCl_4$ in pentane. The cooling bath was removed. The reaction mixture was stirred overnight at room temperature to give a dark brown mixture, which was then brought to dryness under reduced pressure. The dark brown powder was slurried in 100 mL of pentane and transferred into a filtration apparatus equipped with sidearm (to allow solvent refluxing) connecting the system above and below the frit, a receiving flask on the bottom and bubble condenser on the top. The filtered 100 mL of pentane solution was separated and pentane removed to dryness, to yield 3 g of dark solid, which was washed with 20 mL of Et_2O and then dried again to give 0.52 g of pure racemic **Ti-2**. ^1H NMR (δ, ppm, CD_2Cl_2): *t*-Bu, s, 1.38, 18H; $-CH_2-$, s, 4.91, 2H; Cp−H, s, 5.25, 2H; Ar, t, 7.02−7.12, 2H; Ar, d+t, 7.3−7.5, 4H; d, 7.70−7.75, 2H. The remaining solid was extracted with refluxing CH_2Cl_2 for about 3 h. The filtrate was evaporated to dryness under reduced pressure to give 5.0 g of dark powder, which, due to its low purity, was further washed with Et_2O (25 mL) to give 0.54 g of pure product. Combined yield was 14%. Anal. Calcd for $C_{27}H_{30}Cl_2Ti$: C, 68.5; H, 6.4. Found: C, 58.0; H, 6.0.

Synthesis of *rac*-[CH$_2$(3-*t*-BuInd)$_2$]HfCl$_2$ (Hf-2). A 4.16 g sample of bis(1-*tert*-butyl-3-indenyl)methane (98.9% by GC, 11.6 mmol) were dissolved in 80 mL of Et_2O in a 100 mL Schlenk tube, and the solution cooled to 0 °C. A 9.4 mL portion of 2.5 M BuLi in hexane (23.5 mmol) was added dropwise over 5 min with stirring. The solution was allowed to warm to room temperature and stirred for 5 h. An increasing turbidity developed with final formation of an orange suspension. A 3.74 g sample of $HfCl_4$ (Roc-Ric, 99.99% Hf, 11.6 mmol) was slurried in 80 mL of toluene. The two mixtures were both cooled to −20 °C, and the $HfCl_4$ slurry in toluene was quickly added to the Li salt of the ligand in Et_2O. The reaction mixture was stirred for 30 min at −20 °C and then overnight at room temperature (16 h). The orange suspension was filtered over a G4 frit, and the filtrate was brought to dryness under reduced pressure, to yield 4.9 g of a sticky, dark orange product, which was washed with 30 mL of Et_2O. The orange solid so obtained was dried in vacuo to give 3.76 g (54% yield) of pure racemic **Hf-2**. ^1H NMR (δ, ppm, CD_2Cl_2): *t*-Bu, s, 1.37, 18H; $-CH_2-$, s, 4.78, 2H; Cp−H, s, 5.72, 2H; Ar, t, 7.07−7.12, 2H; Ar, t, 7.25−7.35, 2H; d, 7.50−7.57, 2H; d, 7.7−7.8, 2H. Orange crystals of **Hf-2**, suitable for X-ray analysis, were grown from a concentrated toluene solution at −20 °C. Anal. Calcd for $C_{27}H_{30}Cl_2Hf$: C, 53.7; H, 5.0; Hf, 29.6. Found: C, 51.3; H, 5.2; Hf, 28.0 (Zr, 440 ppm).

X-ray Diffraction Structural Analysis. (a) Collection and Reduction of X-ray Diffraction Data. Suitable crystals of **2** and **Hf-2** were mounted in air on a glass fiber tip onto a goniometer head. Single-crystal X-ray diffraction data were collected on a Siemens SMART CCD area detector diffractometer for **2** and on an Enraf-Nonius CAD-4 diffractometer for **Hf-2**, using graphite-monochromatized Mo Kα radiation (λ = 0.71073 Å) at room temperature.

For **2**, unit cell parameters were initially obtained from 156 reflections ($5° < \theta < 20°$) taken from 45 frames collected in three different ω regions and eventually refined against 8192 reflections, while for **Hf-2** the setting angles of 25 randomly distributed intense reflections with $10° < \theta < 14°$ were processed by least-squares fitting.

For **2**, a full sphere of reciprocal space was scanned by 0.3° ω steps, collecting 2400 frames each at 20 s exposure. The detector was kept at 5.00(2) cm from the sample. Intensity decay was monitored by re-collecting the initial 100 frames at the end of data collection and analyzing the duplicate reflections. The collected frames were processed for integration;[16] an empirical absorption correction was made on the basis of 20 142 symmetry-equivalent reflection intensities (SADABS,[17] average redundancy: 4.49).

For **Hf-2** data collection was performed by the ω scan method with variable scan speed (maximum time per reflection 60 s) and variable scan range (0.80 + 0.35 tan θ°). Crystal stability under diffraction was checked by monitoring three standard reflections every 180 min. The measured intensities were corrected for Lorentz, polarization, decay, and background effects and reduced to F_o^2. An emprical absorption correction was applied using ψ scans of three suitable reflections having χ values close to 90°.[18] Crystal data and data collection parameters are summarized in Table 4.

(b) Structure Solution and Refinement. The structures were solved by direct methods[19] and subsequent Fourier synthesis; they were refined by full-matrix least-squares on F^2 [16] using all reflections for **2** and reflections with $I > 2\sigma(I)$ for **Hf-2**. Scattering factors for neutral atoms and anomalous dispersion corrections were taken from the internal library of SHELX97.[20] Weights were assigned to individual observations according to the formula $w = 1/[\sigma^2(F_o^2) + (aP)^2 + bP]$, where $P = (F_o^2 + 2F_c^2)/3$; a and b were chosen to give a flat analysis

(16) *Brucker AXS*; Bruker: Madison, WI, 1996−1999.
(17) Sheldrick, G. M. *SADABS: program for empirical absorption correction*; University of Göttingen: Göttingen, 1996.
(18) North, A. C. T.; Phillips, D. C.; Mathews, F. S. *Acta Crystallogr.* **1968**, *A24*, 351.
(19) Altomare, A.; Cascarano, G.; Giacovazzo, C.; Guagliardi, A.; Burla, M. C.; Polidori, C.; Camalli, M. *J. Appl. Crystallogr.* **1994**, *27*, 435.
(20) Sheldrick, G. M. *SHELX97: program for crystal structure refinement*; University of Göttingen: Göttingen, 1997.

of variance in terms of F_o^2. Anisotropic displacement parameters were assigned to all non-hydrogen atoms. Hydrogen atoms were placed in idealized position ($d_{C-H} = 0.93$, 0.96, and 0.97 Å for aromatic, methylene, and methyl hydrogen atoms, respectively) and refined riding on their parent atom with an isotropic displacement parameter 1.2 times that of the pertinent carbon atom. The correctness of the absolute structure for **Hf-2** was checked, and the Flack parameter[21] for the correct enantiomer was 0.023(14).

The structure of **Hf-2** is affected by a disorder of the toluene solvate molecule. Since it was difficult to refine a consistent disordered model (possibly because of the large volume, 200 Å^3, of the cavity occupied by the toluene molecule), the contribution of the "solvent" was subtracted from the observed structure factor according to the BYPASS[22] procedure, as implemented in PLATON.[23]

The final difference electron density map showed no features of chemical significance, with the largest peaks lying close to the metal atoms. Final conventional agreement indexes and other structure refinement parameters are listed in Table 4.

Polymerizations. Polymerization grade propene and hexane were received directly from the Montell Ferrara plant. MAO was a commercial product (Witco, 10% w/w in toluene, 1.7 M in Al), which was used as received. The catalyst mixture was prepared by dissolving the desired amount of the metallocene with the proper amount of the MAO solution, obtaining a red solution, which was stirred for 10 min at ambient temperature before being injected into the autoclave. A 2 L sample of propene was charged at room temperature in a 4.25 L jacketed stainless steel autoclave, equipped with a magnetically driven stirrer and a 35 mL stainless steel vial, connected to a thermostat for temperature control, previously purified by washing with an Al(*i*-Bu)$_3$ solution in hexanes and dried at 50 °C in a stream of propene. Al(*i*-Bu)$_3$ (1 mmol in hexane) was added as scavenger before the monomer. The autoclave was then thermostated at 2 °C below the polymerization temperature, and then the toluene solution containing the catalyst/cocatalyst mixture was injected in the autoclave by means of nitrogen pressure through the stainless steel vial, the temperature rapidly raised to the polymerization temperature, and the polymerization carried out at constant temperature for 1 h. After venting the unreacted monomer and cooling the reactor to room temperature, the polymer was dried under reduced pressure at 60 °C.

Acknowledgment. We thank S. Tartarini, A. Bellucco, and D. Angeli for the polymerization results, I. Camurati, F. Piemontesi, and M. Colonnesi for the NMR analysis, I. Mingozzi, C. Baraldi, G. Manica, and L. Rimessi for viscosity, solubility, and SEC measurements, F. Testoni, M. Cavallazzi, and P. Marisaldi for the GC−MS analysis, and R. Selleri for the elemental analysis. We also thank Dr. J. Ewen for discussions and Montell for support.

Supporting Information Available: Tables of crystal data, structure solution and refinement, atomic coordinates, bond lengths and angles, anisotropic displacement parameters, an ORTEP figure for **2** and **Hf-2**, and the $\ln[b_{obs}/(1 - b_{obs})]$ versus $1/T_p$ plot of *i*-PP samples made with **2**/MAO and **1**/MAO. This material is available free of charge via the Internet at http://pubs.acs.org.

OM990487O

(21) Flack, H. D. *Acta Crystallogr.* **1983**, *A39*, 876.
(22) van der Sluis, P.; Spek, A. L. *Acta Crystallogr.* **1990**, *A46*, 194.
(23) Spek, A. L. *Acta Crystallogr.* **1990**, *A46*, C34.